Dalton Transactions

Accepted Manuscript

ROYAL SOCIETY OF CHEMISTRY

www.rsc.org/dalton

Cite this: DOI: 10.1039/c0xx00000x

www.rsc.org/xxxxxx

ARTICLE TYPE

$Sr_{7.3}Ca_{2.7}(PO_4)_6F_2$: Eu^{2+}, Mn^{2+} : a novel single-phased white light-emitting phosphor for NUV-LEDs

Jianyan Ding, Quansheng Wu, Yanyan Li, Qiang Long, Chuang Wang and Yuhua Wang*

Received (in XXX, XXX) Xth XXXXXXXXX 20XX, Accepted Xth XXXXXXXXX 20XX

DOI: 10.1039/b000000x

In this study, a series of novel single-phased white light-emitting phosphor $Sr_{(7.3-x/2-y/2)}Ca_{(2.7-x/2-y/2)}(PO_4)_6F_2$: xEu^{2+}, yMn^{2+} ($0 \le x \le 0.06$, $0 \le y \le 0.9$) (SCPF: xEu^{2+}, yMn^{2+}) have been successfully prepared through a high temperature solid-state reaction. The crystal structure and photoluminescence have been measured and analyzed. The energy transfer mechanism is demonstrated to be a quadrupole-quadrupole interaction and the critical distance between the Eu^{2+} and Mn^{2+}has been calculated. Meanwhile, the efficiency η of the energy transfer from Eu^{2+} to Mn^{2+} can reach 76%. The excitation spectra monitored at 457 nm range from 290 nm to 400 nm. Under excitation at 365 nm, the emission spectra include two broad bands peaked at 458 nm and 570 nm. By changing the ratio of Eu^{2+} / Mn^{2+}, the emission color can change from blue to white. Furthermore, our results give the Commission International de L'Eclairage (CIE) chromaticity coordinates for the white LED as (0.334, 0.307) and a correlated color temperature of 3982K, which indicates that the SCPF: Eu^{2+}, Mn^{2+} phosphor is a very promising candidate for near ultraviolet (NUV) white light emitting diode (WLED) phosphor.

1. Introduction

In recent years, WLEDs have attracted much attention and gradually replace the traditional filament lamps to become the next generation solid-state light sources, due to their low energy consumption, long service lifetime, as well as high brightness and environmentally friendly properties.[1,2] Until recently, the commercial WLEDs was achieved by the combination of an InGaN chip with a $Y_3Al_5O_{12}$: Ce^{3+} (YAG: Ce) phosphor. However, this kind of WLEDs exhibits a high correlated color temperature (CCT) and a poor color rendering index duo to a lack of the red emission band.[3-5] In order to overcome this problem, the method of blending tricolor (blue, green, red) phosphors upon the UV chips has been employed to realize warm-WLEDs. However, this way also suffers from the problem of the low luminescence efficiency and color aberration due to emission reabsorption and different degradation rates of the three-primary phosphors.[6-8] Be based upon the status quo, the single-phased white light-emitting phosphors have become more and more important because of their excellent luminescence efficiency, color reproducibility and good color rendering index. In order to get a single-phase white-emitting phosphor with full-color emission, integrating single-doped activators into different crystallographic sites, co-doped activators using energy transfer and Eu^{2+}/ Eu^{3+} -codoped have been employed, such as $Ca_6Y_2Na_2(PO_4)_6F_2$: Eu^{2+}, Mn^{2+},[9] $Sr_3GdNa(PO_4)_3F$: Eu^{2+}, Mn^{2+},[10] $Na_2Ca_4Mg_2Si_4O_{15}$: Eu^{2+}, Mn^{2+},[11] $La_5Si_2BO_{13}$: Ce^{3+}, Mn^{2+},[12] $CaZr(PO_4)_2$: Eu^{2+}/Eu^{3+},[13] Ca_2PO_4Cl: Eu^{2+}, Mn^{2+},[14] $Ca_9Mg(PO_4)_6F_2$: Eu^{2+}, Mn^{2+},[15] and so on.

Fluoro-apatite phosphors with the general formula $M_{10}(XO_4)_6L_2$ (M = Ca, Sr, Ba; X = P, Si, V; L = F, Cl, OH) are widely studied due to their excellent chemical and thermal stability, low resultant temperature, and environmentally friendly[16-19]. Among the apatite-type fluorophosphors family, $Ca_{10}(PO_4)_6F_2$ is the most common fluoro-apatite and has been widely investigated for different applications. Through Sr replacing Ca ions, a novel phase of $Sr_{7.3}Ca_{2.7}(PO_4)_6F_2$ can be formed[20], which is isostructural with the fluorapatite ($Ca_{10}(PO_4)_6F_2$). To the best of our knowledge, the luminescence properties of $Sr_{7.3}Ca_{2.7}(PO_4)_6F_2$ containing rare earths ions have not been reported before. As we know, Eu^{2+} is a good sensitizer because it has strong absorption in the UV and visible region, and high emission intensity due to its d-f dipole-allowed transitions. The emission spectrum is dependent on crystal field and covalency which is attributed to outmost 5d electron, so the emission spectrum of Eu^{2+} ions exhibits a broad band covering blue color to red color. On the contrast, Mn^{2+} ions often act as an activator due to its d-d spin-forbidden transitions. However, Mn^{2+} ions can exhibit a broad emission band in the visible range.[21-23] In order to improve the Mn^{2+}-emission intensity, Eu^{2+} ions act as a good sensitizer, transferring part of its energy to Mn^{2+} ions. In a number of hosts, this way has been employed to realize warn white-emitting.[21-23]In the present work, we synthesized the novel SCPF: Eu^{2+}, Mn^{2+} phosphors by a solid state reaction and its crystal structure and phase analysis have been investigated, through the X-ray powder diffraction (XRD) measurements and the Rietveld structural refinements. The luminescence properties and the mechanism of the energy transfer from Eu^{2+} to Mn^{2+} ions were also discussed in detail.

2. Experimental

2.1 Materials and synthesis

A series of SCPF: Eu^{2+}, Mn^{2+} phosphors were synthesized by a high solid-state reaction method. The raw materials $CaCO_3$ (A. R. (Analytical Reagent)), $SrCO_3$ (A. R.), CaF_2 (A. R.), $NH_4H_2PO_4$ (A.R.), Eu_2O_3 (99.99%) and $MnCO_3$ (A. R.) were added in a stoichiometric ratio. After mixing and ground in an agate mortar, the mixtures were heated at 1250 °C for 4h under a 5% H_2- 45% N_2reducing atmosphere, then the samples were furnace-cooled to room temperature, and ground again into powders for measurement.

2.2 Measurements and characterization

The crystal structures of the synthesized samples were identified by (XRD) using a Rigaku D/max–2400 X diffraction with Ni-filtered Cu Kα radiation. The photoluminescence (PL) and photoluminescence excitation (PLE) were measured by a FLS-920T fluorescence spectrophotometer equipped with a 450W Xe light source and double excitation monochromators. The PL decay curves were measured by a FLS-920T fluorescence spectrophotometer with nF900 nanosecond Flashlamp as the light source. All of the measurements were performed at room temperature.

3. Results and discussion

3.1 Phase identification and crystal structure

In order to investigate the crystal structure of the SCPF, especially for the coordination environment of the Ca^{2+}/Sr^{2+} ions, the Rietveld structural refinements for SCPF were performed based on the general structure analysis system (GSAS) program[24] and the calculated, observed, and different results for the Rietveld refinement XRD patterns are shown in the Fig. 1(a). All of the observed peaks satisfy the reflection condition and converge to R_{wp} = 7.6%, R_p = 6.01%, and χ^2 = 3.801. Fig. 1(b) exhibits that SCPF crystallizes in a hexagonal crystal system with space group P 6_3 (173) and lattice parameters of a = 9.6033Å, c = 7.1309Å, respectively. The exact Rietveld refinement and crystal data of $Sr_{7.3}Ca_{2.7}(PO_4)_6F_2$phosphor are listed in Table 1. It indicates that SCPF is isostructural with the fluorapatite ($Ca_{10}(PO_4)_6F_2$). Meanwhile, the coordination environments of the cation sites are also presented in the Fig. 1(b) and there are two kinds of the cation sites which are occupied by Ca^{2+} and Sr^{2+} ions. One site is coordinated to nine oxygen atoms, and the other is a seven-fold coordinated site which is surrounded by six oxygen atoms and one fluorine atom. As can be seen, two cation sites are connected by five and six tetrahedral PO_4 groups, respectively, through corner shared and edge shared. It is well known that the radii of Eu^{2+} and Mn^{2+} ions are close to that of Ca^{2+} or Sr^{2+} ions.[25]On the basis of the similar effective ionic radii and valence state, we can reasonably suppose that Eu^{2+} and Mn^{2+} ions occupy Ca^{2+} or Sr^{2+} sites at random.

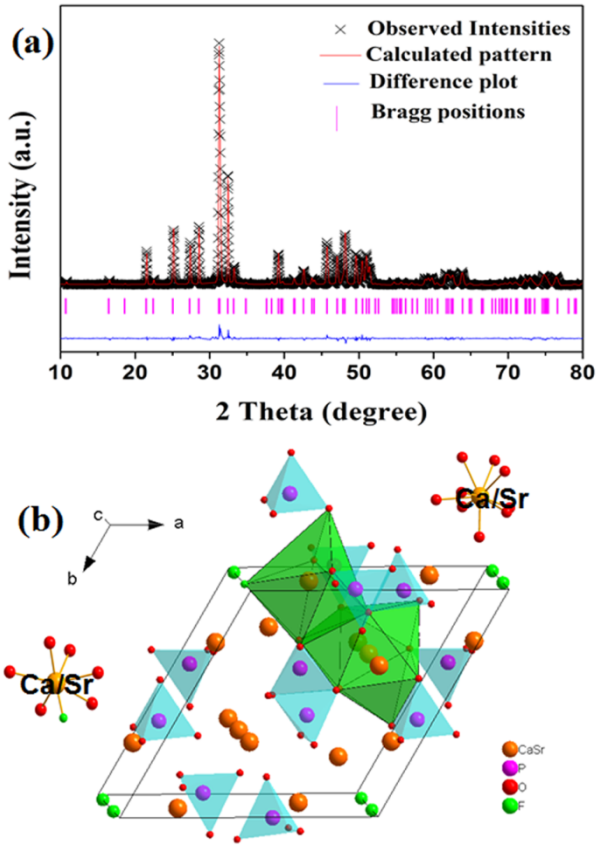

Fig. 1 (a) Rietveld refinement of powder XRD profile of $Sr_{7.3}Ca_{2.7}(PO_4)_6F_2$. (b) Crystal structure of $Sr_{7.3}Ca_{2.7}(PO_4)_6F_2$ and the coordination environment of the Ca^{2+}/Sr^{2+} ions.

Table 1 Rietveld refinement and crystal data of $Sr_{7.3}Ca_{2.7}(PO_4)_6F_2$ phosphor.

Empirical formula	$Sr_{7.3}Ca_{2.7}(PO_4)_6F_2$
Radiation type	Cu Kα
2θ range (˚)	10-80
Formula weight	677.83 g/mol
Crystal system	hexagonal
Space group	P 63 (173)
a/Å	9.6033
c/Å	7.1309
V/Å^3	569.53
Z	2
R_p (%)	6.01
R_{wp}(%)	7.6
χ^2	3.801

Fig. 2 shows the XRD patterns of the obtained SCPF: 0.03Eu^{2+}, $y$$Mn^{2+}$ ($0 \le y \le 0.9$) phosphors with different Mn^{2+} concentration. When the diffraction data were compared with the simulated patterns, it is found that all the positions and relative intensity are in good agreement with the simulated patterns and no impurity phase was detected. The results indicate that the prepared samples belong to the pure phase.

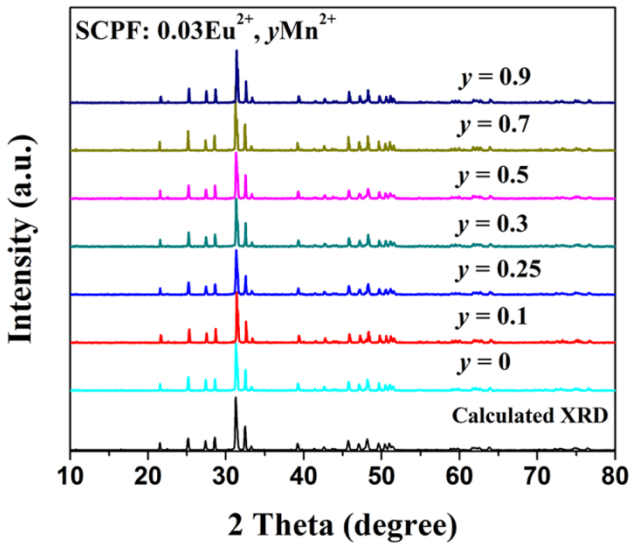

Fig. 2XRD patterns of SCPF: 0.03 Eu^{2+}, yMn^{2+} ($0 \le y \le 0.9$) phosphors and simulated patterns.

3.2 Luminescence properties of Eu^{2+} and Mn^{2+} in the SCPF

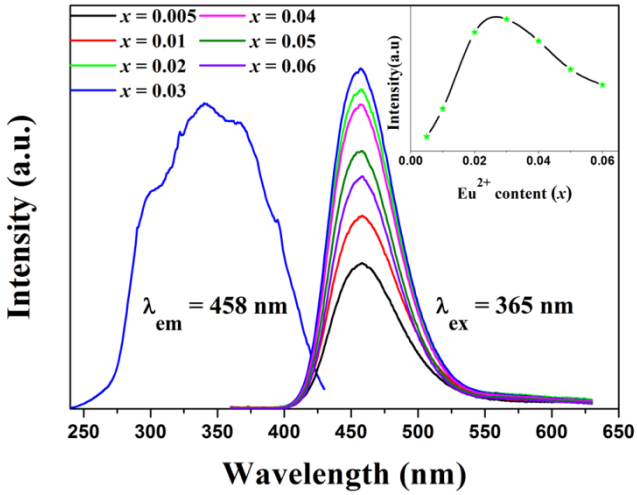

Fig. 3 The emission spectra and excitation spectrum of the SCPF: xEu^{2+} ($0.005 \le x \le 0.06$). The inset exhibits the relationship between the emission intensity of Eu^{2+} ions and doped Eu^{2+} content.

Fig. 3 exhibits the PL spectra of Eu^{2+} activated SCPF. As can be seen, SCPF: Eu^{2+} has a broad excitation band in the range of 290 nm to 400 nm monitoring at 458 nm, which is due to the $4f^7$-$4f^65d^1$ transitions of the Eu^{2+} ions. Under excitation at 341 nm, the blue light peaked at 458 nm can be detected. The asymmetric broad emission band can be deconvoluted into two well-separated Gaussian components peaked at 450 nm and 480 nm, which indicates that there are two luminescence Eu^{2+} centers in the host lattice. The phenomenon is consistent with the fact that Eu^{2+} ions occupy two kinds of cation sites (nine-fold coordinated and seven-fold coordinated sites) in the host. The inset of Fig. 3 shows the emission intensity of SCPF: xEu^{2+} at different Eu^{2+} concentrations excited at 365 nm. As the Eu^{2+} content increases, the intensity of the emission spectra of the SCPF: Eu^{2+} increases gradually and reaches a maximum at $x = 0.03$, and then decreases due to the concentration quenching happening between Eu^{2+} ions, so the optimal concentration of Eu^{2+} ions is located at $x = 0.03$.

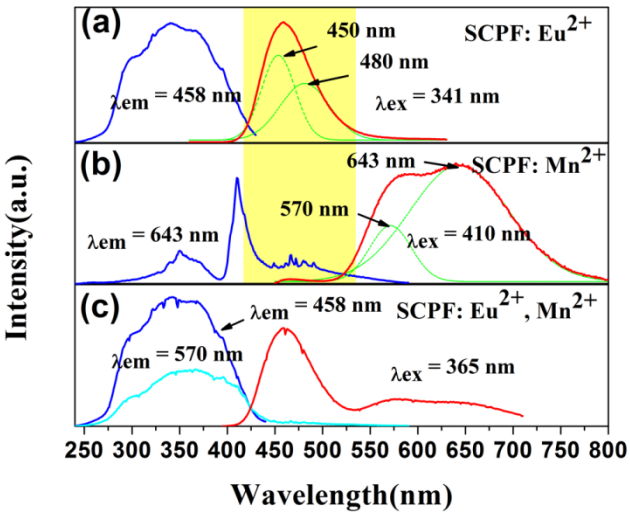

Fig. 4 The excitation spectra (left) and emission spectra (right) of the SCPF: Eu^{2+} (a), SCPF: Mn^{2+} (b), and SCPF: Eu^{2+}, Mn^{2+} (c) samples, and their corresponding Gaussian components (green lines).

Fig. 4(b) displays the PL spectra of SCPF: Mn^{2+}. Monitored at 643 nm, the excitation spectrum show several bands peaking at 280 nm, 335 nm, 404 nm, 495 nm, respectively, corresponding to the transition of Mn^{2+} ions from the ground level $^6A_1(^6S)$ to $^4E(^4D)$, $^4T_2(^4D)$, $[^4A_1(^4G),^4E(^4G)]$ and $^4T_1(^4G)$ excited level, respectively.[26] Under excitation at 410 nm, the SCPF: Mn^{2+} shows a broad emission band ranging from 550 nm to 700 nm, which is attributed to the $^4T_1(^4G)$-$^6A_1(^6S)$ d-d spin-forbidden transition of Mn^{2+} ions. As shown in Fig. 4(b), the asymmetric emission band can be decomposed into two symmetric bands peaked at 570 nm and 643 nm via the Gaussian fitting, A measure of the crystal field strength (Dq) around Mn^{2+} ions can be depicted as follows[27]

$$D_q = \frac{ze^2r^4}{6R^5} \qquad (1)$$

where R is the bond length, z is the anion charge, e is the electron charge, and r is the d wave function. From the Rietveld refinement, we have calculated the average radii of Ca/Sr-O which are 2.6128 Å (CN = 9) and 2.5428 Å (CN = 7). As we know, the Mn^{2+} ions prefer to substitute for the larger Ca^{2+}/Sr^{2+} ions, which could lead to a shortening of the bond length and result in the enhancement of crystal field strength. As a result, the stronger crystal field strength makes the lowest d state of Mn^{2+} ions closer to the ground state and finally produces the red shift.[28] On the basis of the above analysis, the emission peaks located at 570 nm and 643 nm corresponding to the Mn^{2+} occupying seven-fold coordinated sites and nine-fold coordinated sites, respectively.

The PL spectra of Mn^{2+} and Eu^{2+} co-doped SCPF are shown in the Fig. 4(c). Under excitation at 365 nm, the emission band includes two obvious bands peaked at 458 nm belonging to the transition of Eu^{2+} ions and 570 nm attributed to the transition of Mn^{2+} ions. As can be seen, the emission intensity of Eu^{2+} ions is higher than that of Mn^{2+} ions, which is due to the fact that the d-d transition of Mn^{2+} ions is electric spin-forbidden, while f-d transition of Eu^{2+} ions belongs to electric dipole-allowed transition. As shown in Fig. 4(a) and Fig. 4(b), according to the overlap between emission band of the SCPF: Eu^{2+} and the

excitation band of the SCPF: Mn^{2+}, the energy transfer from Eu^{2+} to Mn^{2+} ions is expected to occur. In addition, the excitation spectrum which monitored the emission of the Mn^{2+} ions is consistent with that which monitored the emission of the Eu^{2+} ions, which is another evidence for energy transfer between Eu^{2+} and Mn^{2+} ions.

In order to further understand the energy transfer between Eu^{2+} and Mn^{2+} ions, the emission spectra of SCPF: $0.03Eu^{2+}$, yMn^{2+} ($0 \le y \le 0.9$) excited at 365 nm are presented in the Fig. 5. The Eu^{2+}-content was fixed at 0.03 which is the optimal concentration, while the Mn^{2+}-content changes from 0 to 0.9. As can be seen, the intensity of emission spectra of Eu^{2+} ions decreases monotonically with an increase in Mn^{2+} doping content, whereas the intensity of the Mn^{2+}-emission obviously increases and reaches a maximum at y = 0.6. The concentration quenching happens between Mn^{2+} ions when y> 0.6. According to Paulose et al,[29] the energy transfer efficiency η of the phosphors from Eu^{2+} to Mn^{2+} ions was calculated and can be expressed as in equation:

$$\eta = 1 - I_S/I_{S0} \quad (2)$$

where I_S and I_{S0} are the luminescence intensities of sensitizer Eu^{2+} in the presence and absence of activator Mn^{2+}, respectively. The results are shown in the Fig. 6, as the content of Mn^{2+} increases from 0 to 0.9, the energy transfer efficiency η increases gradually and reaches 76%, when the doping content of Mn^{2+} is 0.7.

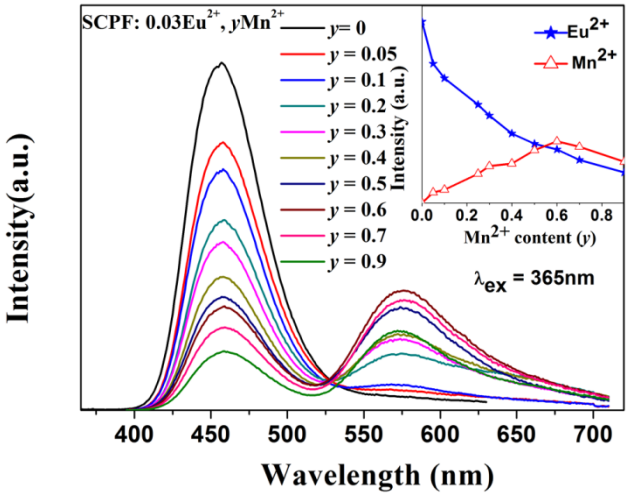

Fig. 5 Emission spectra of the SCPF: $0.03Eu^{2+}$, yMn^{2+} ($0 \le y \le 0.9$) phosphors with various Mn^{2+} content excited at 365 nm. The inset shows the relationship between emission intensity of the Eu^{2+} and Mn^{2+} ions and Mn^{2+} content.

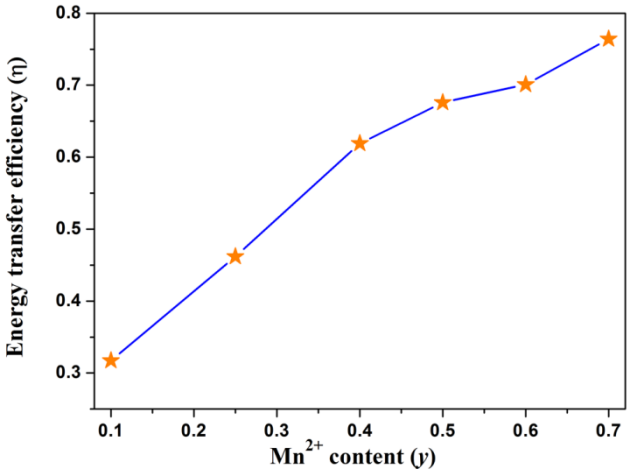

Fig. 6 Dependence of the energy transfer efficiency η using integrated emission intensity on the Mn^{2+} ions content (y).

To further prove the phenomenon that the energy transfer from Eu^{2+} to the Mn^{2+} ions in the SCPF host, the fluorescence decay curves of Eu^{2+} in SCPF: $0.03Eu^{2+}$, yMn^{2+} ($0 \le y \le 0.9$) samples excited at 341 nm, monitored the emission of Eu^{2+} ions at 458 nm were measured and shown in Fig. 7. The decay curves fit well with a second-order exponential decay mode, according to the equation:[30-32]

$$I = A_1 \exp(-\frac{t}{\tau_1}) + A_2 \exp(-\frac{t}{\tau_2}) \quad (3)$$

where I is the luminescence intensity; A_1 and A_2 are constants; t is the time, and τ_1 and τ_2 are rapid and slow times for the exponential components, respectively. The average lifetime τ can be calculated by the formula as follows:[33-35]

$$\tau^* = (A_1\tau_1^{\ 2} + A_2\tau_2^{\ 2})/(A_1\tau_1 + A_2\tau_2) \quad (4)$$

For SCPF: $0.03Eu^{2+}$, yMn^{2+} ($0 \le y \le 0.9$), the calculated average lifetimes (τ^*) are 458.2, 453.3, 416.4, 394.3, 372.3 ns for y = 0, 0.1, 0.4, 0.6 and 0.9, respectively, which are shown in Fig. 7. The phenomenon that the average lifetime τ^* decreases monotonically with increasing Mn^{2+} concentration also indicates energy transfer happening between Eu^{2+} and Mn^{2+} ions.

In order to investigate the mechanism of the energy transfer from the Eu^{2+} to the Mn^{2+} ions, the critical distance R_C of energy transfer from Eu^{2+} to Mn^{2+} ions was calculated using the concentration quenching method. The average separation R_C can be obtained according to the following equation suggested by Blass.[36]

$$R_C = 2[\frac{3V}{4\pi x_C N}]^{1/3} \quad (5)$$

There: x_c is the total concentration of Eu^{2+} and Mn^{2+}, at which the emission intensity of Eu^{2+} is half that of the sample in the absence of Mn^{2+} ions. N is the number of available sites for the dopant in the unit cell (for SCPF, N = 20), and V is the volume of the unit cell (for SCPF, V = 569.53 Å^3). According to the eqn (5), the critical distance R_C was determined to be about 12.19 Å. It is well known that the critical distance between the sensitizer and

activator should be shorter than 5 Å if energy transfer occurs owing to the exchange interaction.[37] Therefore, it is little possibility of energy transfer through the exchange interaction between Eu^{2+} and Mn^{2+} ions.

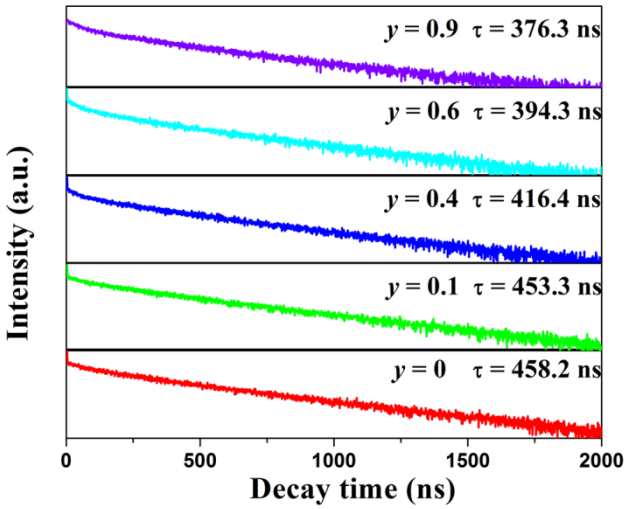

Fig. 7 Decay curves of Eu^{2+} in SCPF: $0.03Eu^{2+}$, yMn^{2+} displayed on a logarithmic intensity scale (excited at 365 nm, monitored at 458 nm).

On the basis of the Dexter energy transfer expression of multipolar interaction and Reisfeld' approximation, the energy transfer mechanism from Eu^{2+} to Mn^{2+} ions in the host should occur via electric multipole-multipole interaction. The following relationship can be adopted by following equation:[38, 39]

$$(\eta_0 / \eta) \propto C^{\alpha/3} \quad (6)$$

where η_0 and η are the luminescence quantum efficiencies of Eu^{2+} in the absence and presence of Mn^{2+}; and α = 6, 8, and 10 corresponds to dipole-dipole, dipole-quadrupole, and quadrupole-quadrupole interactions, respectively. In order to conduct simple assess, the luminescence intensity ratio (I_0/I) is approximately with the value η_0/η as follows:

$$(I_0 / I) \propto C^{\alpha/3} \quad (7)$$

where I_0 and I are the emission intensity of Eu^{2+} in the absence and presence of Mn^{2+}, respectively. The results are exhibited in Fig. 8, which show the I_0/I vs $C_{Eu+Mn}{}^{\alpha/3}$. This clearly indicates a better fitting result for $C^{10/3}$ compared with the others through the linear fitting. This indicates that the quadrupole-quadrupole interaction is mainly responsible for the energy transfer from Eu^{2+} to Mn^{2+} ions.

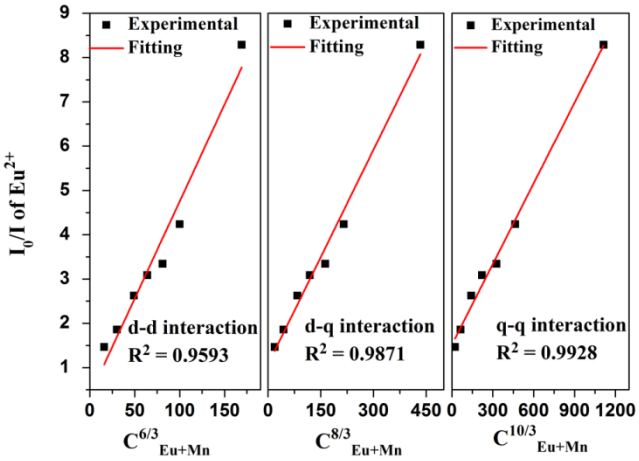

Fig. 8 Dependence of I_0/I of Eu^{2+} on (a) $C^{6/3}$, (b)$C^{8/3}$, (c)$C^{10/3}$.

3.3 CIE coordinates of SCPF: Eu^{2+}, Mn^{2+}

Fig. 9 exhibits the variation of the Commission International de L'Eclairage (CIE) chromaticity coordinates of the SCPF: $0.03Eu^{2+}$, yMn^{2+} phosphors with different Mn^{2+} doping contents, under excitation at 365 nm. The CIE coordinates and CCTs are calculated and summarized in Table 2. The results indicate that the emission light can be modulated from blue to white with the increasing doping content of the Mn^{2+} ions. When the concentration of $Mn^{2+}$is increased to 0.6, a warm white light can be obtained with good CIE coordinates of (0.334, 0.307) and CCT of 3982K. It proves that warm, white light can be realized for practical applications by changing the Mn^{2+} concentration in SCPF: Eu^{2+}, Mn^{2+}.

Table 2 Comparison of the CIE chromaticity coordinates and CCT (K) for SCPF: $0.03Eu^{2+}$, yMn^{2+} phosphors excited at 365 nm.

Sample no.	Sample Composition(n)	CIE coordinates (*x*, *y*)	CCT (K)
1	$y = 0$	(0.155, 0.103)	3042
2	$y = 0.05$	(0.173, 0.129)	4918
3	$y = 0.1$	(0.183, 0.138)	5938
4	$y = 0.25$	(0.251, 0.208)	97050
5	$y = 0.3$	(0.269, 0.234)	21418
6	$y = 0.4$	(0.299, 0.262)	9158
7	$y = 0.5$	(0.334, 0.307)	5402
8	$y = 0.6$	(0.359, 0.331)	4343
9	$y = 0.7$	(0.372, 0.344)	3982
10	$y = 0.8$	(0.369, 0.349)	4129

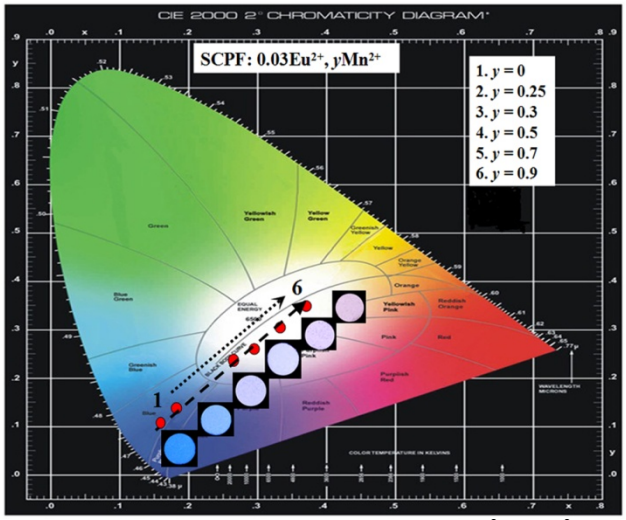

Fig. 9 CIE chromaticity diagram for SCPF: 0.03 Eu^{2+}, yMn^{2+} (y = 0-0.9) phosphors (point 1 to 6) excited at 365 nm.

Conclusion

In summary, a series of the SCPF: Eu^{2+}, Mn^{2+} phosphors were successfully prepared through a solid-state reaction. According to the spectroscopic data and fluorescence decay dynamics, the energy transfer from Eu^{2+} to Mn^{2+} ions via quadrupole-quadrupole interaction have been proved. By adjusting concentration ratio of Eu^{2+} and Mn^{2+}, a warm white light with good CIE coordinates of (0.334, 0.307) and CCT of 3982K can be realized. The results indicate that our identified SCPF: Eu^{2+}, Mn^{2+} phosphors could have a potential value for WLEDs.

Acknowledgements

This work is supported by Specialized Research Fund for the Doctoral Program of Higher Education (no. 20120211130003) and the National Natural Science Funds of China (Grant no. 51372105).

Notes and references

Key Laboratory for Special Function Materials and Structural Design of the Ministry ofthe Education, School of Physical Science and Technology, Lanzhou University,Lanzhou, 730000, China.
**Corresponding author: E-mail: wyh@lzu.edu.cn; Fax: +86-931-8913554; Tel: +86-931-8912772*

[1] S. P. DenBaars, D. Feezell, K. Kelchner, S. Pimputkar, C. C. Pan, C. C. Yen, S. Tanaka, Y. Zhao, N. Pfaff, R. Farrell, M. Iza, S. Keller, U. Mishra, J. S. Speck and S. Nakamura, *Acta Mater.*, 2013, **61**, 945.
[2] L. Chen, C. C. Lin, C. W. Yeh and R. S. Liu, *Mater.*, 2010, **3**, 2172.
[3] C. Hecht, F. Stadler, P. J. Schmidt, J. S. A. der Guenne, V. Baumann and W. Schnick, *Chem. Mater.*, 2009, **21**, 1595.
[4] Z. G. Xia, R. S. Liu, K. W. Huang and V. Drozd, *J. Mater. Chem.*, 2012, **22**, 15183.
[5] W. Z. Lv, Y. C. Jia, Q. Zhao, M. M. Jiao, B. Q. Shao, W. Lu and H. P. You, *Adv. Opt. Mater.*, 2014, **2**, 183.
[6] N. Guo, H. You, Y. Song, M. Yang, K. Liu, Y. Zheng, Y. Huang and H. Zhang, *J. Mater. Chem.*, 2010, **20**, 9061.
[7] W. R. Liu, C. H. Huang, C. W. Yeh, J. C. Tsai, Y. C. Chiu, Y. T. Yeh and R. S. Liu, *Inorg. Chem.*, 2012, **51**, 9636.
[8] W. Lu, Y. C. Jia, Q. Zhao, W. Z. Lv and H. P. You, *Chem. Commun.*, 2014, **50**, 2635
[9] N. Guo, H. P. You, C. Z. Jia, R. Z. O. Yang and D. H. Wu, *Dalton Trans.*, 2014, **43**, 12373
[10] M. M. Jiao, Y. C. Jia, W. Lu, W. Z. Lv, Q. Zhao, B. Q. Shao and H. P. You, *J. Mater. Chem. C*, 2014, **2**, 90
[11] W. Z. Lv, Y. C. Jia, Q. Zhao, M. M. Jiao, B. Q. Shao, W. Lu and H. P. You, *RSC Adv.*, 2014, **4**, 7588
[12] H. K. Liu, L. B. Liao and Z. G. Xia, *RSC Adv.*, 2014, **4**, 7288
[13] J. C. Zhang, Y. Z. Long, H. D. Zhang, B. Sun, W. P. Han and X. Y. Sun, *J. Mater. Chem. C*, 2014, **2**, 312
[14] P. L. Li, Z. J. Wang, Z. P. Yang and Q. L. Guo, *J. Mater. Chem. C*, 2014, **2**, 7823
[15] K. Li, D. L Geng, M. M. Shang, Y. Zhang, H. Z. Lian, and J. Lin, *J. Phys. Chem. C,* 2014, **118**, 11026−11034
[16] I. Mayer, R. Roth and W. Brown, *J. Solid State Chem.*, 1974, **11**, 33.
[17] J. F. Rakovan and J. M. Hughes, *Can. Mineral.*, 2000, **38**, 839.
[18] M. Xie and R. Pan, *Opt. Mater.*, 2013, **35**, 1162.
[19] C. Zhang, S. Huang, D. Yang, X. Kang, M. Shang, C. Peng and J. Lin, *J. Mater. Chem.*, 2010, **20**, 6674.
[20] Pushcharovsky, D. Yu, T. N. Nadezhina and A. P. Khomyakov, *Sov. Phys. Crystallogr.*, 1987, **32**, 524-526.
[21] C. H. Huang, T. M. Chen, W. R. Liu, Y. C. Chiu, Y. T. Yeh and S. M. Jang, *ACS Appl. Mater. Interfaces*, 2010, **2**, 259.
[22] W. R. Liu, C. H. Huang, C. W. Yeh, J. C. Tsai, Y. C. Chiu, Y. T. Yeh and R. S. Liu, *Inorg. Chem.*, 2012, **51**, 9636.
[23] W. R. Liu, C. H. Huang, C. W. Yeh, Y. C. Chiu, Y. T. Yeh and R. S. Liu, *RSC Adv.*, 2013, **3**, 9023.
[24] A. C. Larson and R. B. Von Dreele, *General Structure Analysis System. LANSCE, MS-H805, Los Alamos, New Mexico*, 1994.
[25] R. D. Shannon, Acta Crystallogr., Sect. A: Cryst. Phys., Diffr., Theor. Gen. Crystallogr., 1976, **32**, 751–767.
[26] L. A. Shi, Y. L. Huang and H. J. Seo, *J. Phys. Chem. A*, 2010, **114**, 6927.
[27] P. D. Rack and P. H. Holloway, *Mater. Sci. Eng.*, 1998, **21**, 171−219.
[28] J. Lü, F. Du, R. Zhu, Y. Huang and H. J. Seo, *J. Mater. Chem*. 2011, **21**, 16398−16405.
[29] P. I. Paulose, G. Jose, V. Thomas, N. V. Unnikrishnan and M. K. R. Warrier, *J. Phys. Chem. Solids*, 2003, **64**, 841
[30] C. H. Huang and T. M. Chen, *J. Phys. Chem. C*, 2011, **115**, 2349.
[31] C. H. Huang, T. M. Chen, W. R. Liu, Y. C. Chiu, Y. T. Yeh and S. M. Jang, *ACS Appl. Mater. Interfaces*, 2010, **2**, 259.
[32] W. Lv, W. Lü, N. Guo, Y. Jia, Q. Zhao, M. Jiao, B. Shao and H. You, *Dalton Trans.*, 2013, **42**, 13071.
[33] R. Yu, H. M. Noh, B. K. Moon, B. C. Choi, J. H. Jeong, K. Jang, H. S. Lee and S. S. Yi, *Mater. Res. Bull.*, 2014, **51**, 361.
[34] Z. Xia, J. Zhuang and L. Liao, *Inorg. Chem.*, 2012, **51**, 7202.
[35] Z. Xia, J. Zhuang, A. Meijerink and X. Jing, *Dalton Trans.*, 2013, **42**, 6327.
[36] G. Blasse, *Philips Res. Rep.*, 1969, **24**, 131.
[37] G. Blasse and B. C. Grabmaier, *Luminescent Materials*, *Berlin, Springer*, 1994.
[38] P. I.Paulose, G.Jose, V.Thomas, N. V.Unnikrishnan, M. K. R.Warrier, *J. Phys. Chem. Solids,* 2003, **64**, 841−846.
[39] E. Song,W. Zhao, G. Zhou, X. Dou, H. Ming, C. Yi, *Curr. Appl. Phys*. 2011, **11**, 1374−1378.